Time-dependent cracking in reinforced concrete beams and slabs

R. Ian GILBERT
Professor and Head, School of Civil and Environmental Engineering
The University of New South Wales
Sydney, Australia

Summary

The mechanisms of cracking and the factors affecting the time-varying width and spacing of flexural cracks in reinforced concrete members are examined. Laboratory tests on twelve reinforced concrete beams and slabs subjected to sustained service loads were conducted in order to measure and quantify the effects of steel area, steel stress, bar diameter, bar spacing, concrete cover, concrete strength and concrete shrinkage on the extent of flexural cracking and the width of flexural cracks both immediately after loading and in the long-term after almost 400 days under load. In addition, an analytical procedure is presented that models time-dependent cracking. Use is made of the *tension chord model* developed by Marti et al. [1] and here modified to study the tensile zone of a flexural member and the time-dependent effects of creep and shrinkage.

Keywords: Cracking ; crack width ; crack spacing ; creep ; deformation ; shrinkage ; restraint ; reinforced concrete ; time-dependent behaviour ; laboratory tests.

Introduction

Excessive cracking, resulting from either restrained deformation or external loads, is one of the most common causes or damage in concrete structures and results in huge annual cost to the construction industry. Current design procedures to control cracking using conventional steel reinforcement are overly simplistic and often fail to adequately model the gradual increase in crack widths with time due to the effects of shrinkage.

Bonded reinforcement in a beam or slab restrains shrinkage and imposes a significant tensile force on the concrete at the level of the steel - often significant enough to cause time-dependent cracking. When a flexural member is also restrained at the supports, shrinkage causes a build-up of tension in the member and may result in cracking in previously uncracked regions. Shrinkage also causes a gradual widening of flexural cracks with time.

The width of a crack depends on the quantity, orientation and distribution of the reinforcing steel crossing the crack and the cover to the reinforcement. It also depends on the bond characteristics between the concrete and the reinforcement bars at and in the vicinity of the crack. A local breakdown in bond immediately adjacent to a crack complicates the modeling, as does the time-dependent change in the bond characteristics caused by drying shrinkage.

In this paper, an investigation of flexural cracking under sustained service loads is reported. Crack widths and crack spacings are reported from laboratory tests on 12 beams and slabs subjected to sustained loads for periods up to 400 days in order to quantify the effects of steel area, steel stress, bar diameter, bar spacing, concrete cover and concrete shrinkage. In addition, a reliable design model utilizing the *tension chord model* of Marti et al. [1] is presented and is shown to be suitable for predicting the time-varying width and spacing of cracks caused by bending and shrinkage.

2. The Flexural Cracking Model

Consider a segment of a singly reinforced concrete beam of rectangular section subjected to an in-service bending moment, M_s, greater than the cracking moment, M_{cr}. The spacing between the primary cracks is s, as shown in Fig.1a. A typical cross-section between the cracks is shown in Fig. 1b and a cross-section at a primary crack is shown in Fig. 1c. In Fig. 1d, the cracked beam is idealized as a compression chord of depth kd and width b and a cracked tension chord consisting of the tensile reinforcement (A_{st}) surrounded by an area of tensile concrete (A_{ct}). The centroids of A_{st} and A_{ct} are assumed to coincide at a depth d below the top fibre of the section.

For the sections containing a primary crack (Fig. 1c), A_{ct} = 0 and the depth kd and the second moment of area about the centroidal axis (I_{cr}) may be determined from a cracked section analysis. Away from the crack, the area of the concrete in the tension chord of Fig. 1d (A_{ct}) is assumed to carry a uniform tensile stress (σ_{ct}) which develops due to the bond stress (τ_b)that exists between the tensile steel and the surrounding concrete.

For the tension chord, the area of concrete between the cracks, A_{ct}, may be taken as

$$A_{ct} = 0.5(D-kd)b^* \le 3(D-d)b^* \qquad (1)$$

where b^* is the smaller of b and $m(1\text{-}k)d$; and m is the number of tensile bars. At each crack in the tension chord of Fig. 2d, $\sigma_{st1} = T/A_{st}$ and $\sigma_c = 0$, where

$$T = \frac{nM_s(1-k)d}{I_{cr}} A_{st} \qquad (2)$$

As distance x from the crack increases, the stress in the steel reduces due to the bond shear stress τ_b between the steel and the surrounding tensile concrete. For reinforced concrete under service loads, where σ_{st1} is less than the yield stress f_{sy}, Marti et al. [1] assumed a rigid-plastic bond shear stress-slip relationship, with $\tau_b = 2f_{ct}$ at all values of slip. f_{ct} is the direct tensile strength of concrete. In reality, the magnitude of τ_b is affected by steel stress, concrete cover, bar spacing, transverse reinforcement (stirrups), lateral pressure, degree of compaction, and size of bar deformations. In addition, τ_b is likely to be reduced by shrinkage. Experimental observations indicate that τ_b reduces as the stress in the reinforcement increases. The assumptions made in Eq. 3 lead to predictions of crack widths and crack spacings in reasonable agreement with experimental observations.

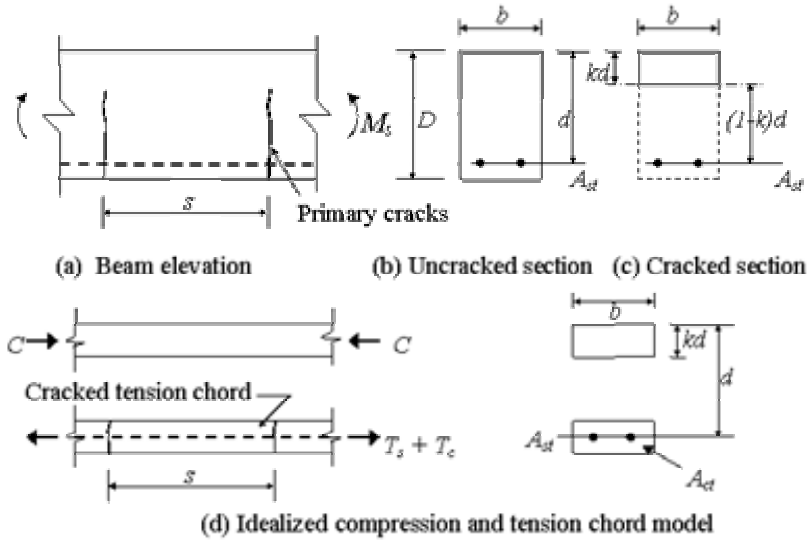

Fig. 1 Cracked r.c. beam and tension chord model.

It is here assumed that

$$\tau_b = \alpha f_{ct} \qquad (3)$$

where, in the short-term,

α = 3.0 when $\sigma_{st1} \le 170$ MPa
α = 2.0 when $\sigma_{st1} > 170$ MPa

and, in the long-term,

α = 1.5 when $\sigma_{st1} \le 170$ MPa
α = 1.0 when $\sigma_{st1} > 170$ MPa.

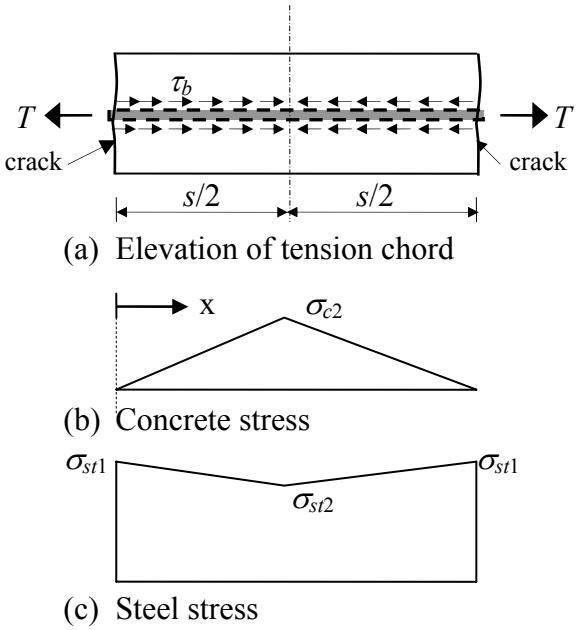

Fig. 2 Tension chord – actions and stresses

Following the approach of Marti et al. [1], the concrete and steel tensile stresses in Figs. 2b and 2c, where $0 < x \le s/2$, may be expressed as

$$\sigma_{stx} = \frac{T}{A_{st}} - \frac{4\tau_b x}{\phi} \quad \text{and} \quad \sigma_{cx} = \frac{4\tau_b \rho\, x}{\phi} \tag{4}$$

where $\rho = A_{st}/A_{ct}$. Midway between cracks, where $x = s/2$, the stresses are

$$\sigma_{st2} = \frac{T}{A_{st}} - \frac{2\tau_b s}{\phi} \quad \text{and} \quad \sigma_{c2} = \frac{2\tau_b \rho\, s}{\phi} \tag{5}$$

The maximum crack spacing $s = s_{max}$ will occur when $\sigma_{c2} = f_{ct}$, and from Eq. 5,

$$s_{max} = \frac{f_{ct}\phi}{2\tau_b \rho} \tag{6}$$

and the minimum spacing is $s = s_{min} = s_{max}/2$. The actual crack spacing s may be expressed as [1],

$$s = \lambda\, s_{max} \qquad \text{where } 0.5 \le \lambda \le 1.0\,. \tag{7}$$

The instantaneous crack width w_i is the difference between the elongation of the tensile steel over the length s and the elongation of the concrete between the cracks and is given by

$$w_i = \frac{s}{E_s}\left[\frac{T}{A_{st}} - \frac{\tau_b s}{\phi}(1 + n\rho)\right] \tag{8}$$

Under sustained load, additional cracks occur between widely spaced cracks (usually when $0.67 s_{max} < s \le s_{max}$). These additional cracks are probably due to the combined effect of tensile creep rupture and shrinkage. As a consequence, the crack spacing reduces with time. The final maximum crack spacing s^*_{max} is only about ⅔ of that given by Eq. 6, but the final minimum crack spacing remains about ½ of the value given by Eq. 6.

As indicated in Eq. 3, experimental observations indicate that τ_b decreases with time, probably as a result of shrinkage induced slip and tensile creep. Hence, the stress in the tensile concrete between the cracks gradually reduces. Further, although creep and shrinkage will cause a small increase in the resultant tensile force T in the real beam and a slight reduction in the internal lever arm, this effect is relatively small and is here ignored in the tension chord model. The final crack width is the elongation of the steel over the distance between the cracks minus the extension of the concrete caused by σ_{cx} plus the shortening of the concrete between the cracks due to shrinkage. For a final crack width of s^*, the final crack width is

$$w^* = \frac{s^*}{E_s}\left[\frac{T}{A_{st}} - \frac{\tau_b s^*}{\phi}(1 + \bar{n}\rho) + \varepsilon_{sh} E_s\right] \tag{9}$$

where ε_{sh} is the shrinkage strain in the tensile concrete; $\bar{n} = E_s/E_e$; E_e is the effective modulus given by $E_e = E_c/(1+\varphi_{cc})$; and φ_{cc} is the creep coefficient of the concrete. If $s^* = s^*_{max} = 0.67\, s_{max}$ (s_{max} is given by Eq. 6), a good estimate of the maximum final crack width is given by Eq. 9.

3. The Experimental Program

3.1. Test specimens and test parameters

A more comprehensive description of the experimental program is available elsewhere [2]. A total of 12 prismatic singly reinforced concrete specimens (6 beams and 6 slabs) with cross-sections shown in Fig.3 were simply-supported over a span of 3.5m and subjected to sustained service loads for periods up to 400 days. In addition to self-weight, the 6 beams were subjected to two sustained point loads (2 x P) each located at the third span points and the 6 slabs were each subjected to a sustained uniformly distributed superimposed load (q). The load on all specimens was sufficient to cause primary cracks to develop in the region of maximum moment.

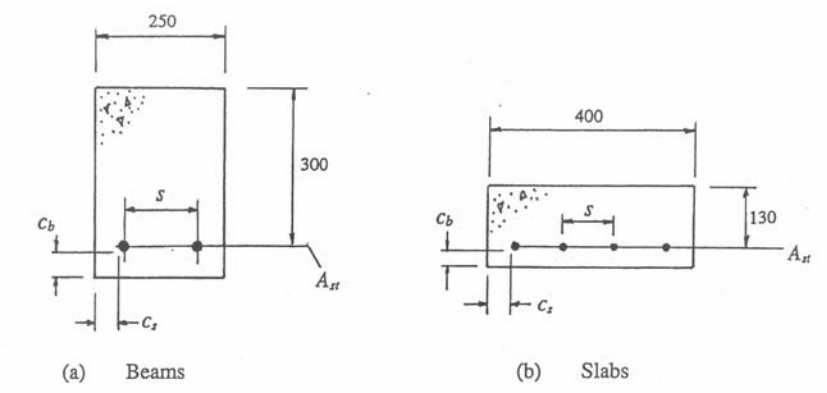

Fig. 3 Details of specimen cross-sections.

All specimens were cast on the same day from the same batch of concrete and moist cured prior to the commencement of the tests at age 14 days.

Details for each specimen are given in Table 1 and Table 2. Also given is the sustained in-service moment at midspan, M_s, the calculated ultimate flexural strength, M_u, the calculated cracking moment, M_{cr}, and the ratio M_s/M_u.

Table 1 Details of beam specimens

Specimen	No. of bars	Bar dia . (ϕ)(mm)	Load, P (kN)	c_b (mm)	c_s (mm)	s (mm)	M_{cr} (kNm)	M_s (kNm)	M_u (kNm)	M_s/M_u (%)
B1-a	2	16	18.6	40	40	150	14.0	24.9	56.2	44.3
B1-b	2	16	11.8	40	40	150	14.0	17.0	56.2	30.2
B2-a	2	16	18.6	25	25	180	13.2	24.8	56.2	44.1
B2-b	2	16	11.8	25	25	180	13.2	16.8	56.2	29.8
B3-a	3	16	27.0	25	25	90	13.7	34.6	81.5	42.4
B3-b	3	16	15.2	25	25	90	13.7	20.8	81.5	25.5

Table 2 Details of slab specimens

Specimen	No. of bars	Bar dia. (ϕ)(mm)	UDL,q (kN/m)	c_b (mm)	c_s (mm)	s (mm)	M_{cr} (kNm)	M_s (kNm)	M_u (kNm)	M_s/M_u (%)
S1-a	2	12	2.9	25	40	308	4.64	6.81	13.58	50.1
S1-b	2	12	1.9	25	40	308	4.64	5.28	13.58	38.9
S2-a	3	12	4.9	25	40	154	4.74	9.87	19.84	49.7
S2-b	3	12	2.9	25	40	154	4.74	6.81	19.84	34.3
S3-a	4	12	5.8	25	40	103	4.84	11.25	25.73	43.7
S3-b	4	12	3.9	25	40	103	4.84	8.34	25.73	32.4

The properties of the concrete at various ages after casting were measured from companion cylinders and prisms using standard test procedures and are given in Table 3. The creep coefficient for concrete first loaded at age 14 days, φ_{cc}, and the shrinkage strain, ε_{sh}, were measured on 300 mm diameter cylinders and slab specimens 160 mm thick, respectively, and are given in Table 4.

Table 3 Properties of Concrete

Material Property	Age (days)			
	7	14	21	28
Compressive strength (MPa)	12.9	18.3	23.1	24.8
Flexural tensile strength (mod. of rupture) (MPa)	3.0	3.7	4.3	5.6
Indirect tensile strength (split cylinder) (MPa)		2.0	2.6	2.8
Modulus of elasticity (MPa)	21090	22820	23990	24950

Table 4 Measured creep coefficient and shrinkage strain

Age (days)	14	16	21	27	53	96	136	200	242	332	394
φ_{cc}	0	0.14	0.36	0.48	0.92	1.15	1.29	1.40	1.50	1.64	1.71
ε_{sh} (x 10^{-6})	0	14	109	179	403	591	731	772	784	816	825

3.2. Measured crack spacing and crack width – Discussion and comparison of results

The measured average crack spacings and crack widths immediately after first loading and at age 400 days are given in Tables 5 and 6. The measurements were taken at the bottom fibre of each specimen on all cracks in the middle third of the beams (where the moment was nearly constant) and over the middle third of the slab (where the moment exceeded 90% of its value at mid-span). The maximum, minimum and average crack widths are recorded. Complete details of the crack patterns and the full set of results are reported in [2].

At first loading, a regular pattern of primary cracks developed in each member. With time, the cracks gradually increased in width and additional cracks developed between some of the original cracks. All beam specimens (with 16 mm diameter bars) had average instantaneous crack spacings of between 200 and 240 mm, with the exception of B2-b. For the slabs, with 12 mm bars, the average instantaneous crack spacing was between 135 and 145 mm, with the exception of S1-b. Under sustained load, the average crack spacing reduced significantly, with the final crack spacing for all beams in the range 129-194 mm and for all slabs in the range 95-128 mm.

A comparison of results for beams B1-a and B2-a and beams B1-b and B2-b shows the influence of concrete cover. Immediately after first loading, the crack widths are larger for the beam with the largest cover, as expected. However, in the long-term the maximum crack widths are less dependent

Table 5 Crack widths and spacings immediately after first loading (Age 14 days)

Specimen	Experimental Results				Analytical Predictions		
	Avge crack spacing (mm)	Crack width (mm)			Crack spacing (mm)		Maximum crack width (mm)
		Avge. w_{avge}	Min. w_{min}	Max. w_{max}	Min	Max	
B1-a	231	0.11	0.06	0.13	167	335	0.16
B1-b	227	0.04	0.02	0.05	112	223	0.05
B2-a	201	0.07	0.05	0.10	158	316	0.16
B2-b	315	0.04	0.03	0.05	105	210	0.05
B3-a	230	0.05	0.03	0.08	99	199	0.13
B3-b	232	0.04	0.03	0.05	66	132	0.03
S1-a	136	0.05	0.03	0.08	85	170	0.14
S1-b	189	0.05	0.02	0.08	85	170	0.09
S2-a	136	0.10	0.05	0.13	76	152	0.13
S2-b	138	0.07	0.05	0.08	76	152	0.07
S3-a	144	0.08	0.05	0.10	70	139	0.10
S3-b	142	0.05	0.03	0.08	70	139	0.06

Table 6 Crack widths and spacings at Age 400 days

Specimen	Experimental Results				Analytical Predictions		
	Avge crack spacing (mm)	Crack width (mm)			Crack spacing (mm)		Maximum crack width (mm)
		Avge. w_{avge}	Min. w_{min}	Max. w_{max}	Min	Max	
B1-a	165	0.28	0.10	0.38	167	223	0.38
B1-b	194	0.13	0.10	0.18	112	149	0.20
B2-a	129	0.20	0.13	0.36	158	210	0.36
B2-b	181	0.11	0.03	0.18	105	140	0.19
B3-a	130	0.17	0.06	0.28	99	132	0.23
B3-b	133	0.09	0.03	0.13	66	88	0.11
S1-a	121	0.15	0.05	0.20	85	113	0.22
S1-b	115	0.09	0.05	0.15	85	113	0.18
S2-a	97	0.15	0.05	0.23	76	102	0.19
S2-b	95	0.11	0.03	0.18	76	102	0.15
S3-a	111	0.15	0.10	0.25	70	93	0.16
S3-b	128	0.13	0.08	0.20	70	93	0.14

on cover. Shrinkage appears to increase slip between the concrete and the steel and render the cracks more parallel sided. Hence, the dependency of crack width on cover is reduced with time.

Also shown in Tables 5 and 6 are the predicted crack spacings and maximum crack widths calculated using the flexural cracking model of Section 2. Considering the inherent variability of cracking, agreement between the predicted and observed values is good, both immediately after loading and after prolonged periods under sustained loading.

Concluding Remarks

A design model is presented for predicting the time-varying width and spacing of cracks caused by bending and shrinkage in reinforced concrete flexural members. Also presented are the results from laboratory tests on 12 beams and slabs subjected to sustained service loads for periods up to 400 days. The crack widths and crack spacings calculated using the analytical design model are in good agreement with the experimental observations.

Acknowledgements

The support of the Australian Research Council is gratefully acknowledged. The author wishes to thank Mr S. Nejadi for assisting with the experimental program.

References

[1] MARTI P., ALVAREZ M., KAUFMANN W., and SIGRIST V., "Tension Chord Model for Structural Concrete", Structural Engineering International 4/98, 1998, pp 287-298.

[2] NEJADI S. and GILBERT R.I., "Flexural Cracking in Reinforced Concrete Members – an Experimental Study", (in preparation).